nature communications

Article

https://doi.org/10.1038/s41467-025-61520-8

Global alternatives of natural vegetation cover

Received: 9 September 2024

Accepted: 25 June 2025

Published online: 16 July 2025

Check for updates

Jean-François Bastin[1] ✉, Nicolas Latte[1], Jan Bogaert[1], Claude A. Garcia[2,3], Fabio Berzaghi[4,5], Fernando T. Maestre[6], Jens-Christian Svenning[7], Emeline Assede[8,9], Sabas Barima[10], Timothée Besisa[1,11], Samuel Bouchoms[1], Thomas W. Crowther[12], Thalès de Haulleville[13], Hugo de Lame[1], Pauline Depoortere[1], Marc Dufrêne[1], Anne J. Hoek Van Dijke[14], Simon Lhoest[1], Gregory Mahy[1], Christian Messier[15,16], Danilo Mollicone[17], Felana Nantenaina Ramalason[1,18], Marc Peaucelle[19], Antoine Plumacker[1], Fabien Quétier[20], Olivia Rakotondrasoa[18], Kouagou Raoul Sambieni[1,21], Ben Sparrow[22], Yegor Tarelkin[1], Yannick Useni Sikuzani[23], Arthur Vander Linden[1] & Philippe Lejeune[1]

Preserving and restoring terrestrial ecosystems is essential to preventing the decline of life on Earth. To guide global conservation efforts, we present a detailed counterfactual map showing Earth's natural tree, short vegetation, and bare ground cover. This map accounts for environmental filtering along with realistic scenarios of fire frequency and wildlife herbivory. The most likely scenario suggests 43% (5669 ± 74 Mha) of land could support trees, 39% (5183 ± 86 Mha) shrubs and grasses, and 18% (2352 ± 59 Mha) bare ground. Adjustments in fire and herbivory could shift a minimum of 675 Mha of land, stressing the importance of considering alternative outcomes when restoring a landscape. Our findings also suggest that adjustments in fire frequency and wildlife herbivory could have a greater impact on natural vegetation than expected climate changes by 2050, highlighting decision-makers' responsibility to guide conservation and restoration toward a sustainable and biodiverse future.

During the last decades, several planetary boundaries have been crossed, including those related to biosphere integrity and climate change[1]. These highlight the urgent need to halt and reverse the loss of biodiversity in order to achieve safe living conditions on Earth[2–6]. International organizations have recognized this urgency, as reflected by the adoption by the General Assembly of the United Nations, on the 1st of March 2019, of a resolution to establish the 2021-2030 period as the "Decade of Ecosystem Restoration". This resolution is also backed by the latest reports of the 6th Assessment Report of the Intergovernmental Panel on Climate Change[2], the adoption of global quantitative restoration targets under the Global Biodiversity Framework by the parties of the Convention on Biological Diversity in Montréal in December 2022, and the adoption of the European Nature Restoration law in June 2024. However, among the key scientific challenges to responsible ecosystem conservation and restoration is understanding the natural baseline conditions of any region, and the natural states that are possible for any plot of land.

While ecosystem restoration is largely supported by governments, NGOs and stakeholders in ecosystems across the globe, restoration actions on the ground have often focused disproportionately on planting trees through reforestation or afforestation, even in areas that were not naturally forested[7,8]. Such bias toward tree planting could lead to unintended consequences for the mitigation of climate change, the conservation of other life

A full list of affiliations appears at the end of the paper. ✉e-mail: jfbastin@uliege.be

forms (including vegetation, animals, fungi, and microbes), and the rights and livelihoods of local communities[9]. Examples of negative unwanted impacts include, but are not limited to, warming in boreal regions due to tree cover-induced changes in albedo[10], increased evapotranspiration leading to a loss of water availability[11], lower carbon storage in soils when replacing old-growth grasslands with tree plantations[12], or a collapse in native biodiversity with the replacement of native savannahs by exotic plantations[7]. To minimize these risks of damaging land conversion, socially and ecologically responsible land management strategies require a fundamental understanding of the natural state of ecosystems across the globe.

A growing body of research highlights the potential for natural restoration (i.e. ecosystem restoration practices that involve minimal human intervention) to maximize healthy biodiversity outcomes[13,14]. But successful natural restoration requires a basic understanding of the diversity of natural ecosystem states that can be found within a given landscape, so that different habitat types and maximum biodiversity can be preserved[15]. In this context, grasslands and shrubland ecosystems must not only be considered as degraded or temporary alternatives to forests (as has occurred in several mass plantation examples), but, where appropriate, as climax ecosystems in their own right[16,17], with the necessary consideration of the various mechanisms (including fire and herbivory) shaping the formation of open ecosystems[18,19]. It is crucial to move beyond a narrow focus on "forest vs. non-forest" possibilities and to explore a wider range of potential natural land cover diversity accounting for the risks and benefits that may arise from various natural restoration targets[20]. While recognizing the importance of considering diverse ecosystems for restoration is not new in restoration ecology[14,21,22], (Materials and methods are available as supplementary materials) we still lack a comprehensive assessment of the different possible natural states of ecosystems across the globe that would be critical for guiding national and international land management policies, as well as their implementation on the ground[7–9].

Results and discussion

Here, we generate, to our knowledge, the first map of the potential natural states of broad vegetation types, showing the most probable natural land cover in every pixel across the globe. These broad ecosystem categories include tree cover (tall woody vegetation), short vegetation (shrubs and grasses), and bare ground (areas devoid of perennial vegetation but which might harbor biocrusts and annual plants) at a resolution of 0.25° (Fig. 1). This map, referred to as the global natural vegetation cover, is generated using data collected over 40,000 0.5-hectare plots systematically distributed within all protected areas (Fig. S1; "Methods"). To predict the different natural vegetation cover, we trained models using photo-interpreted vegetation cover data from protected areas and predicted natural variation using climate variables, soil properties, fire frequency, and wildlife herbivory within a neural network modeling framework ("Environmental determinants of land cover" in "Methods"). Using possible scenarios of fire and herbivory at the ecoregion or biome level ("Environmental determinants of land cover" in "Methods"), we aimed to explore the possible mechanisms that might have the greatest potential for establishing natural vegetation states in different regions across the globe. We then generated the final counterfactual map by extrapolating the model beyond protected areas. We refer to this map as "counterfactual" as it illustrates the natural vegetation cover carrying capacity of the planet, i.e. a different situation of current actual vegetation cover that can be mapped directly from satellites[23].

The central challenge in our analysis is identifying "natural" reference state of any ecosystem. We chose protected areas as the best representation of the most natural state of our ecosystems. Many protected areas experience some level of human degradation that might ultimately lead our model to the misrepresentation of the reference state. Degradation can relate to historical and current anthropogenic activities like legal and illegal logging, past defaunation and local extinctions, ongoing poaching or excessive hunting, or increased abundance of exotic pests and diseases[24–26]. To limit the potential resulting bias, we further extrapolate our map considering as

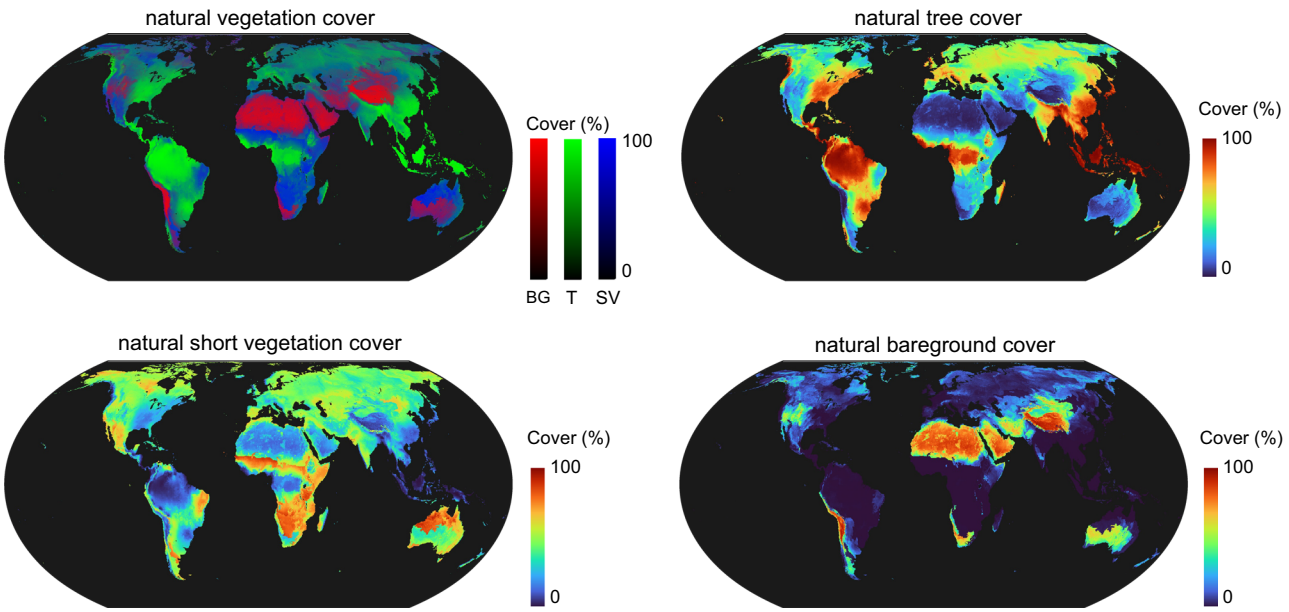

Fig. 1 | The global natural vegetation cover. The map displays the global natural vegetation cover per pixel as for 2015 according to a median scenario of fire and herbivory, based on the observed fire regime and herbivory per ecoregion within protected areas of IUCN class I, II, and III. The sum of potential tree (T), short vegetation (SV), and bareground (BG) cover (top left) equals 100% for each pixel. The remaining subfigures display each potential land cover separately for enhanced clarity. The color gradient highlights large contrasts and should be interpreted with caution detailed information for visualization at the pixel level is available here: https://bastinjf-climate.users.earthengine.app/view/gavcglobalfractionalvegetationmedian.

https://doi.org/10.1038/s41467-025-61520-8

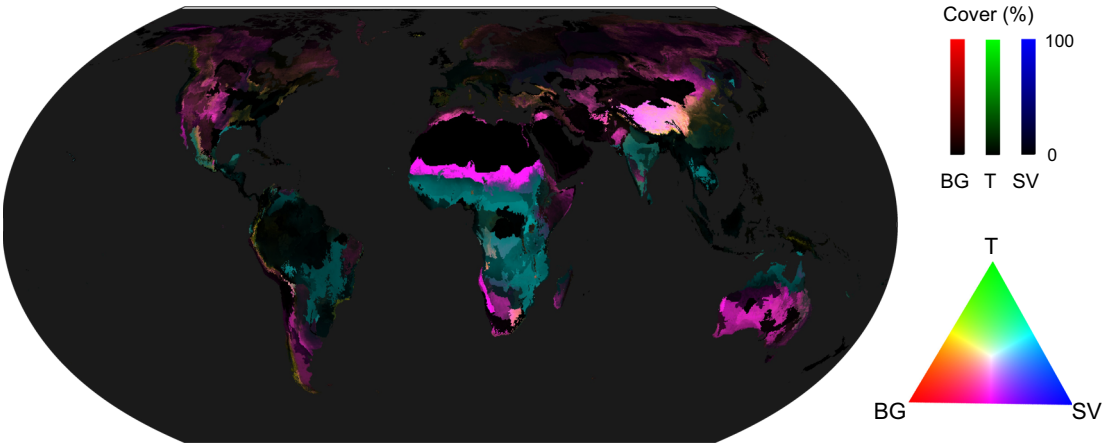

Fig. 2 | Global alternatives of natural vegetation cover. This map depicts the natural alternatives of vegetation cover on a global scale as for 2015, based on the changes in fire regime (prescribed or excluded) and herbivore intensity scenarios. Each pixel of the map represents the standard deviation (SD) of the predictions for bare ground (BG), tree (T), and short vegetation (SV) cover. The resulting additive color rendering corresponds to pixels where alternatives are found between two dominant land cover types (cyan for trees and short vegetation, magenta for short vegetation and bare ground, and in yellow for trees and bare ground). A Venn diagram summarizes this color legend. The color gradient highlights large contrasts and should be interpreted with caution detailed information for visualization at the pixel level is available here: https://bastinjf-climate.users.earthengine.app/view/gavcglobalalternativescenarios.

a reference state solely those protected areas under conservative IUCN categories I, II, and III (i.e. over 17,000 plots; "Augmented Visual Interpretation" in "Methods"). The spatial distribution of the remaining protected areas might also lead to the misrepresentation of the global alternatives of natural vegetation cover, due to spatial aggregation and misrepresentation of global environmental conditions. To this end, we control for the spatial structure using spatial blocks for cross validation[27] ("model training and control of spatial structure" in "Methods"), and validate their environmental representativity using spatial features approach[28,29] ("The representativity of the training dataset" in "Methods"). All the models yielded good results (observed vs. predicted $R^2 \geq 0.8$; average intercept of 0.04 ranging from 0 to 0.07 and average slope = 0.97 ranging from 0.92 to 1), showing a very limited impact (<1%) of the modelling framework and of the choice of climate dataset and a rather limited (~5%) impact of the spatial structure of the training dataset ("The neural network model" in "Methods"). We then generated the final counterfactual map by extrapolating the model beyond protected areas for each climate data source and calculating the mean natural vegetation cover for each pixel, using the most probable (i.e., median) scenario of fire and herbivory ("Environmental determinant of land cover" in "Methods"). We employed various climate databases to account for the model's sensitivity to the choice of climatic data and accounted for potential model overfitting. The control of spatial feature distributions shows that our calibration dataset is well representative of the global dataset ("The representativity of the training dataset" in "Methods").

The global natural vegetation cover

Our study reveals that the most probable global natural vegetation cover of the planet (Fig. 1) is comprised of 5669 (±74) Mha of trees (43%), 5183 (±86) Mha of short vegetation (39%), and 2352 (±59) Mha of bare ground (18%). Our counterfactual map reveals two distinct patterns at the global level (Fig. 1). From tropical to desert regions, each biome tends to be dominated by a single type of vegetation cover. Tropical biomes are dominated by trees, subtropical biomes by short vegetation, and desert biomes by bare ground (Table S1). From temperate to boreal regions, each biome tends to present a more balanced distribution of the natural vegetation cover offering more opportunities in terms of land management. This finding is in line with a recent assessment of the state of European land cover during the last interglacial period, which showed that Europe was covered by heterogeneous and complex landscapes in the youngest period with a similar climate as today and absence of *Homo sapiens*[30]. Tropical and subtropical moist forests have the largest area naturally covered by trees (on average 1616 Mha), but also present 312 Mha of land naturally covered by short vegetation. Similarly, tropical and subtropical grasslands have the largest area naturally covered by short vegetation (1127 Mha), but also present 722 Mha of land naturally covered by trees. Desert biomes, while dominated by bare ground (1300 Mha) might also shelter a significant area of natural short vegetation and tree cover, with 1053 Mha and 419 Mha respectively. The carrying capacity for natural vegetation in desert biomes is expected to decline over the coming decades due to forecasted climate and land use changes[4,31]. Boreal and temperate biomes exhibit high carrying capacities for both short vegetation and tree cover, with temperate biomes supporting 1095 Mha of short vegetation and 1341 Mha of tree cover, and boreal biomes supporting 656 Mha of short vegetation and 717 Mha of tree cover.

These results highlight that landscape restoration cannot afford to overlook any type of land cover. Whether in arid, boreal, temperate, or tropical biomes, a restoration project should always consider the opportunity, costs, and benefits of restoring different ecosystems, and the possibility of letting restored natural processes determine the outcome. This underscores the remarkable heterogeneity of vegetation on Earth and the intricate challenges associated with their conservation and restoration.

Global alternatives of natural vegetation cover

Using multiple realistic fire frequency and wildlife herbivory scenarios, i.e. from percentile 5th to 95th in the observed range of fire frequency and herbivore biomass in each ecoregion of the world, we map all the potential alternatives of natural land cover on Earth (Fig. 2). Each pixel of the map represents the standard deviation of the predictions obtained from the different scenarios for tree, short vegetation, and bare ground cover in green, blue, and red respectively (Fig. 2). The resulting additive color rendering corresponds to landscapes where diverse natural vegetation cover can be found. In total, the map illustrates that at least 675 Mha of the Earth's surface can support alternative vegetation covers, an area equivalent to the size of the Amazonian bassin[32] ("Map of the global alternative natural vegetation cover and sensitivity to fire and herbivory scenarios" in "Methods"). The most substantial hotspots where alternative natural vegetation

occur in subtropical and temperate biomes, where fire and herbivory scenarios promote the transition from dense forests to grassy systems and eventually from grassy systems to deserts (Fig. 2). These hotspots result mostly from an asymptotic relationship between land cover and fire regime, as an increase of fire will substantially favor short vegetation over trees beyond a certain threshold of fire frequency ("The neural network model" in "Methods"). The effect of wildlife herbivory appears more complex, as an increase of herbivory biomass is not systematically related to a decrease of tree cover. Indeed, high herbivore densities can be found both within dense forests (e.g., forest elephants, great apes, etc.) and herbaceous savannas[33]. High herbivore densities can also increase vegetation heterogeneity and consequently their overall resilience vs. external forcing[34]. Further development of the method at finer scales might benefit from a focus on the potential effect of trait-specific herbivores to better identify the effect of herbivores on the landscape[35]. Also, wetlands are not included in the modeling process, even though they may contain trees, short vegetation, and barren land. Since conservation or restoration choices could significantly impact wetland ecosystems, we emphasize that they should be carefully considered when assessing alternative options for natural vegetation cover. Here, we estimate that less than 5% of wetlands could be affected by these alternatives, warranting a thorough evaluation of potential outcomes using existing wetland maps for guidance[36].

Our counterfactual maps provide valuable insights to help guide ecosystem restoration efforts, accounting for a full range of natural options in terms of vegetation cover that together shape complex and heterogeneous landscapes[37]. The maps and the model we built can assist decision-makers, policy makers, and local stakeholders in assessing how climate change, prescribed fire intensity, fire exclusion, and wildlife herbivory may affect the tree, short vegetation, and bare ground cover of a given landscape. This could help guiding existing restoration initiatives such as natural grazing projects in Europe's rewilding landscapes, where we can evaluate the scenario needed to promote more heterogeneous landscapes[15] and address the effects of, for instance, land abandonment[38], trophic rewilding experiments in Siberia (e.g. "the Pleistocene park") where grassy ecosystems might stabilize soil temperatures and limit permafrost melting[39], trophic rewilding experiments in African savannah where elephants help promote semi-open ecosystems[40], or reforestation initiatives in Africa aiming to slow down land degradation and desertification (e.g., the Great Green Wall[41]).

The role of fire and herbivory in shaping vegetation

Using our model considering various fire frequency and herbivory scenarios, together with the average expected climate change by 2050[42], we found that an increase of herbivore biomass up to 30,000 kg perkm²—i.e. close to the upper limit observed in Europe latest interglacial age[43] or about 30 bisons or six elephants per km²—can decrease the tree cover from 55% to 11% in the Dinaric mountains of Europe, and from 44% to 8% in the Northeast Siberian Taiga (Fig. 3). Fire prescription or exclusion in West Sudanian savannah might change the potential tree cover by 23%, shifting between 33% and 56% when passing from 0.5 to 0 fire yr^{-1} (Fig. 3). Interestingly, results show that the choice of management action appears to have a much stronger impact on the final land cover than average climate change alone. In this regard, the effects of the average expected climate change by 2050 only changed the resulting land cover of the previous examples by less than 3%. While the maps and model presented here are robust and informative and provide a global picture of the different potential natural alternatives, further refinement and validation of our models would enhance their accuracy and usefulness for specific restoration or rewilding initiatives on the ground. Future refinements should notably consider incorporating additional biogeographical variables, such as more detailed climate-derived indices and improved spatial data on soil properties and hydrology[44–46], while also refining disturbance modeling—particularly fire and herbivory—by integrating finer-scale dynamics of herbivore biomass, functional diversity, intake rates, and fire regimes across different ecological contexts[24,47,48]. The inclusion of punctual but extreme climatic events such as extreme drought[49] or tropical cyclones[50] might also improve our understanding of the effect of climate change vs. the effect of management action on the resulting land cover.

In conclusion, our model reveals the considerable potential for diverse natural vegetation states across the globe. Given the critical differences in ecosystem states that are possible, our findings highlight that land management actions might outweigh the average effect of climate change on the restoration outcome. As such, we believe that our results can help guide the design of ecologically and socially responsible landscape conservation and restoration initiatives that are required to combat the ongoing climate and biodiversity crises.

Methods

The raw data and the complete annotated code (including data preparation, model training, validation, and evaluation, and mapping) used in the present study are available on GitHub (https://github.com/Nicolas-Latte/GANVC).

Set-up of the study

We set-up a data-driven neural network model to map the Earth´s natural fractional vegetation cover. The model is trained on climatic, topographic, edaphic, herbivory, and fire data in combination with a dataset of land-cover in protected areas of the globe. We used this model to predict the natural fractional vegetation cover beyond protected areas.

Assessment of land cover

The training dataset corresponds to the augmented photo-interpretation of three types of land cover: trees, short vegetation (including grasses and shrubs), and bare ground. We used data from 40,520 0.5-hectare plots distributed across the protected areas of the globe (Fig. S1) and following a systematic sampling grid design (20 by 20 km). This dataset results from previous studies on the global assessment of dryland forests and the global tree restoration potential and corresponds to the land cover of 2015[4,51].

Augmented visual interpretation of the three land covers

The assessment of land cover in each plot was conducted using the Augmented Visual Interpretation approach with the assistance of Collect Earth[52]. Collect Earth, an open-access software developed by the Open Foris initiative of the Food and Agriculture Organization of the United Nations (FAO), utilizes Google Earth and Google Earth Engine to provide multi-source and multi-level information to facilitate the photo-interpretation of land cover. This software enables the operator to perform photo-interpretation of a 70 × 70 m square plot, combining land cover information derived from satellite images with very high spatial (pixel size ≤ 1 m) and temporal (daily data acquisition) resolution.

To interpret the land cover, the operator utilizes freely accessible, very high spatial resolution satellite images which can be visualized on Google Earth. Simultaneously, the operator cross-references the interpretations with spectral information obtained from medium-to-high resolution satellite images, including MODIS, Landsat 7/8 from USGS mission, and Sentinel 2 from Copernicus mission, which have been automatically compiled over the past 20 years. In our case, each plot consists of a systematic grid of 7-by-7 points (49 points), allowing convenient and direct estimations of tree cover, short vegetation cover, and bare ground cover. Each point on the grid represents 2% of the plot area.

https://doi.org/10.1038/s41467-025-61520-8

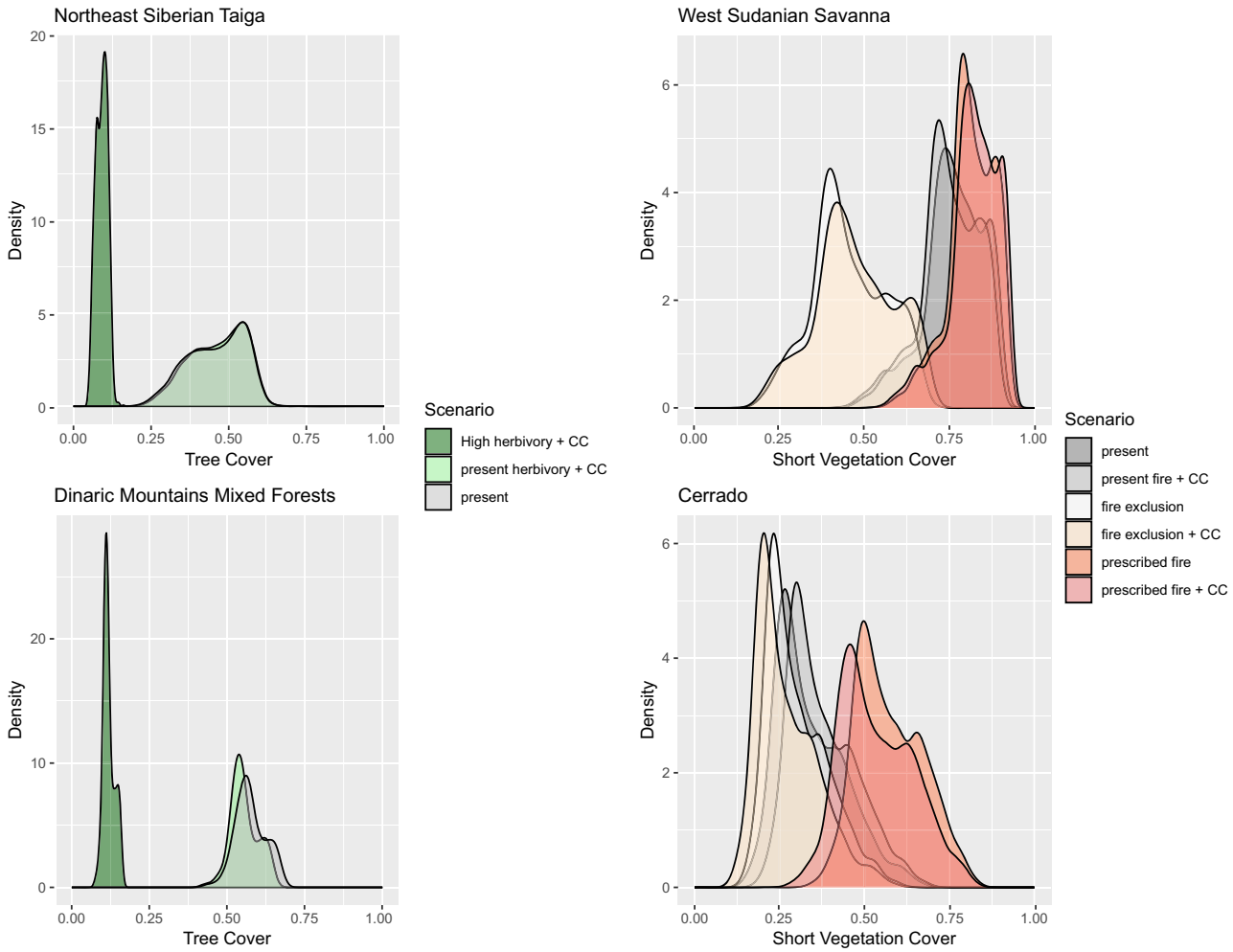

Fig. 3 | Examples of natural vegetation cover distribution variations resulting from different fire, herbivore, and climate change scenarios at the ecoregion level. The effect of fire, herbivory, and climate change SSP5 [CC] is illustrated on the potential tree cover of four ecoregions, i.e., the Northeast Siberian Taiga, the Dinaric Mountains Mixed Forests, the West Sudanian Savanna, and the Cerrado. The two panels on the left compare the potential natural tree cover in current situation vs. low/high herbivory (30 tons.ha^{-1}) and expected climate change by 2050. The two panels on the right compare the current situation vs. fire prescription (+0.25 fire.yr^{-1})/ exclusion (0 fire.yr-1) and expected climate change by 2050.

The three land covers range from 0 to 100% and sum up to 100% for each plot. Distinguishing trees from short vegetation was based on visual assessment of crown size, where crowns width below 2 meters considered as non-tree woody cover. This dataset and approach have been validated on multiple occasions with ground control points[51,53]. More details on the photo-interpreted methodology and inventories we use are provided in previous studies[4,51,53,54].

Environmental determinants of land cover

To build the global distribution of the three land covers and the subsequent global alternatives of natural vegetation cover map, we further develop an empirical model based on neural network approaches[55] to predict the relationship between environmental determinants (climate, topography, soil, fire regime, and wildlife herbivory) and land cover within protected areas. We detail hereafter the preprocessing of each of the datasets used and the selected predictive variables.

Protected areas. We identified regions of the world with limited human activity using the World Database on Protected Areas[56] (WDPA), developed by the United Nations Environmental Program (UNEP) and the International Union for Conservation of Nature (IUCN). These regions are nonetheless not entirely exempt from human activity[26]. Therefore, we distinguish conservative protected areas from the rest. Among the 40,520 plots, two categories were defined. Category 0: 17,638 plots falling under conservative IUCN categories I, II, and III. Category 1: 22,882 plots falling under IUCN categories IV, V, and VI. Model training was done with both categories with a specific predictive variable expressing the category but maps were produced considering only the restrictive IUCN categories I, II, and III (thus category 0) to estimate the natural vegetation cover of the planet with limited human activity.

Climate data. In the present study, we consider that global climate databases, whether derived from meteorological station records or satellite mission predictions, are prone to uncertainties and biases[57]. To address this potential issue, we have incorporated six global climate reference datasets, namely CHELSA, CRU (TS4), ERA5, MODIS, NEX historical, and Worldclim[58–62].

For each climate dataset, we computed four predictive climate variables: the mean and standard deviation of monthly average temperatures, and the mean and standard deviation of monthly total precipitation. Monthly temperatures and precipitations were computed over a significant time span of 10 to 30 years, between 1980 and 2010, depending on the availability of the data in each specific dataset. The selected climate variables capture both the annual average conditions and the seasonal patterns.

Soil and topography. As in Bastin et al., 2019[4], we selected five predictive variables derived from soilgrids[63] and GMTED2010[64]: soil organic carbon stock from 0-to-15 cm, depth to bedrock, sand content from 0-to-15 cm, elevation, and hillshade.

Fire frequency. We computed fire frequency using the Terra and Aqua combined MCD64A1 Version 6 Burned Area MODIS data product[65]. It is a monthly, global gridded 500 m product containing per-pixel burned-area and quality information. The MCD64A1 burned-area mapping approach employs 500 m MODIS Surface Reflectance imagery coupled with 1 km MODIS active fire observations. Here, we converted the map into binary yearly information, counting whether a fire was detected or not each year of the period 2001–2020. We then computed a single map to assess the yearly fire frequency over the 2000–2020 period.

Herbivory. The herbivory dataset is compiled from the study of Berzaghi et al., of 2024[66], where the authors studied the global distribution of wild mammal herbivore biomass using dynamic vegetation models calibrated on observed datasets gathered over protected areas. To account for the general trends of herbivore biomass and daily intake in natural systems, we merged the data, that was originally structured in 24 functional groups, into three levels of information, i.e. the estimated dry biomass in kilogram of wet weight per km^2 (i.e., the biomass), the estimated total biomass intake in kg of dry mass· per km^2 (i.e., the intake) and, finally, the estimated daily litter intake in kg of dry mass per square kilometer. Accounting for the litter intake allows focusing on the impact of herbivores being very dependent on the seasonal source of intake (i.e. the litter).

The herbivore data being the result of a model, it presents some potential shortcomings, in particular regarding the definition of natural vs. domestic mammals that might differ depending on the perspective of the stake holder[67]. Therefore, the risk of considering non-native herbivore biomass in protected areas is non-null in our model. Yet, as functional type of herbivore—not nativeness—is what matters in terms of impact on the land cover[35], we assume that such bias has little impact on the result of our model which only considers the impact of herbivore intensity on the potential state of vegetation.

List of all the predictive variables. Based on aforementioned steps, we select a total of 14 variables (Fig. S2): protected area category (0: I, II, III and 1: IV, V and VI), mean of precipitation, mean of temperature, standard deviation of precipitation, standard deviation of temperature, bedrock depth, elevation, hillshade, soil organic carbon content, sand content, fire frequency, herbivore total biomass, herbivore total intake, and herbivore litter intake.

The representativity of the training dataset

To assess the representativity of the training dataset, we first analyze the ranges of the environmental variables within and outside protected areas per biomes (Fig. S3). The protected areas cover well the global variation of environmental data. Additionally, to assess statistically the representativity of the training dataset, we performed a nearest neighbor distance analysis in feature spaces following recommendations of Meyer and Pebesma[28]. The results in Fig. S4 illustrate the good representativity of the training dataset.

As a final test of data representativity, we compare results obtained using the full range of available data in protected areas with those derived from data restricted to Categories I, II, and III protected areas (Supplementary Note 1, Figs. S5, S6).

The neural network model

Neural network architecture. Our model is a simple neural network, i.e., a MultiLayer Perceptron (MLP). The model is composed of a first linear transformation (14 predictive variables -> 64 features) followed by a "tanh" activation function and a dropout of 0.75, then a second linear transformation (64 features -> 3 proportions). At the end of the MLP, we applied a "softmax" activation function to reconstruct proportions of the three land covers: trees, short vegetation, and bare ground (sum of proportions = 1). The total number of parameters is 1155. Input and output data are tabular with one line per photo-interpreted plot for training and one line per pixel of 0.25° (world) for prediction.

Model training and control of spatial structure. As well as the MLP, we configurated the training to avoid model overfitting and ensure prediction robustness. We set the training parameters (number of epochs = 3000, learning rate = 0.001, weight decay = 0.001, etc.) through trial and error. In total, we trained 66 MLPs: 10 (spatial folds) +1 (all folds) for each of the six climate datasets. We used the weighted mean square error (MSE) as loss function (Fig. S7). We weighted the loss for balancing the number of samples between continents, IUCN categories (0/1), and vegetation cover classes (highest proportion). The 10 folds correspond to spatially and environmentally separated areas (Fig. S8), generated using the blockCV package in R[27].

Model evaluation. We validated the model progressively by analyzing the residuals and the variable importance of the predictive variables and their model profiles. The comparison of predicted and observed values (Fig. S9) revealed that the models generally present a good and unbiased prediction ($R^2 \geq 0.8$; average intercept of 0.04 ranging from 0 to 0.07 and average slope = 0.97 ranging from 0.92 to 1), yet with a small systematic underestimation of the prediction of high bare ground values.

The predictive power of the 14 selected variables is high. We performed a first assessment through the averages and ranges of the model profiles (Fig. S10). This figure shows how, at the global level, each land cover responds to the variation of standardized model parameters. Interestingly, and despite being an empirical machine-learning model, the figure presents biologically meaningful relationships between the predictive and the response variables, providing confidence in the quality of the model. We also performed a second assessment through a variable importance analysis (Fig. S11).

Fire regime and herbivory

To model the natural vegetation cover beyond the geographic limits of the world's protected areas, it was necessary to consider potential scenarios of fire regime and herbivory that are currently not present outside protected areas, i.e., counterfactuals. To consider realistic situations, we propose scenarios based on the observed frequency distributions of fire and herbivory within protected areas, calculated for each ecoregion and each biome. For each distribution, we identified 5 intensities: very low (5th percentile), low (25th percentile), median (50th percentile), high (75th percentile), and very high (95th percentile).

The scenarios of fire regime and wildlife herbivory are built from observations within protected areas and are considered per biome and terrestrial ecoregion—as defined by Olson and colleagues[68]-, as these consist of large units of land containing distinct natural communities and species. We therefore assume that the fire regime and the wildlife herbivory observed within the protected areas of these biomes/ecoregions are realistic scenarios of fire and herbivory that could be implemented for a restoration project at the scale of the biomes/ecoregions.

Maps, uncertainties, and confidence intervals of the global natural vegetation cover

Model uncertainties. To capture four sources of mapping uncertainties, we produced 720 maps by combining the 66 models with different prediction configurations:

- The model uncertainty: we estimated the inherent uncertainty of the models by predicting 10 times each of the 6 climate dataset models (all folds) with the dropout activated. Number of maps: 10 repetitions × 6 climates = 60.
- The spatial uncertainty: we estimated the effect of spatial structure of the training dataset by predicting 10 times each of the 6 climate dataset models (10 different folds, deactivated dropout). Number of maps: 10 folds × 6 climates = 60.
- The climate uncertainty: we estimated the effect of the climate dataset on the land cover proportions by predicting one map per climate dataset model (all folds and deactivated dropout). Number of maps: 6 climates = 6.
- We estimated the overall uncertainty by considering 600 combinations: 10 repetitions (activated dropout) × 10 folds × 6 climates (Fig. S12).

All the 720 maps were produced by considering the median (50th percentile) fire and herbivory intensities. Uncertainty values were finally computed as the standard deviation per source and per land cover (Fig. S13). For model and spatial uncertainties, we computed the mean of climate maps before standard deviation (mean: 60 - > 10, sd: 10 - > 1). All maps produced in this study have 3 bands, one per cover.

The global natural vegetation cover map. We computed the global natural vegetation cover as the mean of 6 maps. One map per climate dataset model (deactivated dropout, all folds, and median fire and herbivory scenarios) (Fig. S14).

This map represents the most probable distribution of the three natural vegetation covers: bare ground (red), tree (green), and short vegetation (blue) (Fig. 1). In this study, we did not consider water bodies as potential land for vegetation cover. Antarctica and permanently ice-covered regions of Greenland were excluded from the natural vegetation cover map.

Confidence Intervals. We first estimate the variance for the area covered by each vegetation type by multiplying the standard deviation value of each pixel by the pixel area and summing all pixels at global level. The confidence interval is then calculated by considering the following equation:

$$\mathrm{CI}_i = z^* \frac{\sigma_i}{\sqrt{\mathrm{n}}}$$

Considering a confidence interval of 95%, z equals 1.96; σ corresponds to the area concerned by the uncertainty of the vegetation cover i, and n (the number of land cover maps) equals 600.

The resulting confidence interval equals 59 Mha for the prediction of the natural bare ground cover, 74 Mha for the prediction of the natural tree cover, and 86 Mha for the prediction of the natural short vegetation.

Map of the global alternative natural vegetation cover and sensitivity to fire and herbivory scenarios

Fire and herbivory scenarios sensitivity. The effects of fire and herbivory scenarios can be tested by predicting maps with different configurations of fire and herbivory intensities (no dropout, all folds). In total we produced 150 maps: 5 fire scenarios x 5 herbivory scenarios x 6 climates.

Global alternatives of natural vegetation cover. We produced the global alternatives of natural vegetation cover map (Fig. 2) from the 150 maps by computing the mean of climate maps (150 - > 25) followed by the standard deviation (25 - > 1) (Fig. S15). To estimate the area of land that can shift from one vegetation cover to another from shifts in herbivory and fire intensity, we sum the pixels area concerned by alternative cover multiplied by the highest standard deviation observed per pixel (one of the three land cover type). This resulted in the estimation of a minimum of 675 Mha of land where vegetation cover can be adjusted from herbivory and fire intensity.

Uncertainty vs. scenarios

To compare the effect of uncertainties (model, spatial and climate) to the effect of fire and herbivory scenarios on the natural vegetation cover, we computed the absolute difference between the global map and the other average maps (10 for model uncertainty, 10 for spatial uncertainty, 6 for climate uncertainty and 25 for scenarios). The boxplot of these differences is available in Fig. S16. The variability of areas affected by the scenarios appears much more important than variations due to uncertainties. Yet, the variability associated with the spatial structure should not be neglected.

Other datasets

Focus on wetlands. We assessed global alternatives of natural vegetation cover in wetland by extracting the results of Fig. 2 over global wetland cover as estimated for 2022 by Zhang and colleagues and scaled at 1 km[36].

Climate change. To consider climate change (CC), supplementary predictions were done using "NEX historical" model[69] but with "NEX 2050" data. The climate data for 2050 were computed by averaging values of all models in the NEX CMIP6 product (i.e. ACCESS-CM2", "ACCESS-ESM1-5", "BCC-CSM2-MR", "CESM2", "CESM2-WACCM", "CMCC-CM2-SR5", "CMCC-ESM2", "CNRM-CM6-1", "CNRM-ESM2-1", "CanESM5", "EC-Earth3", "EC-Earth3-Veg-LR", "FGOALS-g3", "GFDL-CM4", "GFDL-ESM4", "GISS-E2-1-G", "HadGEM3-GC31-LL", "HadGEM3-GC31-MM", "IITM-ESM", "INM-CM4-8", "INM-CM5-0", "IPSL-CM6A-LR", "KACE-1-0-G", "KIOST-ESM", "MIROC-ES2L", "MIROC6", "MPI-ESM1-2-HR", "MPI-ESM1-2-LR", "MRI-ESM2-0", "NESM3", "NorESM2-LM", "NorESM2-MM", "TaiESM1", "UKESM1-0-LL") under the scenario ssp5 (Fig. 3).

Statistical analysis synthesis, and reproducibility

We implemented a data-driven modeling approach using a fully connected neural network (multi-layer perceptron, MLP) to predict natural fractional vegetation cover across the globe, divided into three classes: tree cover, short vegetation (shrubs and grasses), and bare ground. The model was trained on 40,520 systematically sampled plots located in protected areas, where vegetation cover was photo-interpreted using high-resolution satellite imagery and the Collect Earth platform. Each plot's cover was annotated as three proportional values summing to 1.

The model utilized 14 predictor variables representing climate, soil, topography, fire frequency, and herbivore biomass and intake. To account for uncertainties in climatic inputs, we trained the model on six global climate datasets (e.g., CHELSA, CRU, ERA5), each with 11 MLP configurations (10 spatial folds and one full training run), totaling 66 models. Spatial structure was addressed using environmentally stratified blocks during training and cross-validation. Training employed a weighted mean squared error loss to correct for imbalances across continents, IUCN categories, and dominant vegetation types. To mitigate overfitting, dropout regularization (rate = 0.75) was applied, and training hyperparameters (e.g., learning rate, epochs) were optimized iteratively.

Model performance was evaluated through predicted–observed comparisons ($R^2 \geq 0.8$) and analyses of variable importance and response profiles. We derived the final global map of natural vegetation cover as the mean prediction across six climate-specific models (all folds, no dropout) under a median scenario of fire and herbivory intensities (i.e., the most probable value of fire intensity), defined per biome and ecoregion from observed percentiles in protected areas.

To quantify prediction uncertainty, we produced 720 model outputs varying climate datasets, dropout settings, and spatial folds, and computed pixel-wise standard deviations per vegetation type. Confidence intervals for area estimates were computed by propagating pixel-level uncertainties and applying a 95% confidence threshold ($z = 1.96$, $n = 600$). We further evaluated sensitivity to fire and herbivory intensities by producing 150 additional maps combining five fire and five herbivory scenarios (5th, 25th, 50th, 75th, 95th percentiles) across six climate datasets. A map of alternative vegetation states was generated from these scenarios using the standard deviation across predictions, and the spatial extent of areas with high variability was calculated. Finally, we compared the magnitude of vegetation shifts driven by fire and herbivory to expected changes under 2050 climate scenarios and assessed impacts on global wetlands using spatial overlays with recent wetland distribution datasets.

All the raw data and the statistical processing can be reproduced from the shared GitHub folder[70].

All analysis were performed using Google Earth Engine and R version 4.4.3; all maps were produced on R version 4.4.3 or on QGIS version 3.40.

Inclusion and ethics statement

The study involved scientists from different parts of the globe (North and South), the contribution of everyone was recognized through co-authorship.

Reporting summary

Further information on research design is available in the Nature Portfolio Reporting Summary linked to this article.

Data availability

The data and the maps are available on a dedicated Github repository: https://github.com/Nicolas-Latte/GANVC (https://doi.org/10.5281/zenodo.15480101[70]) or upon request to the corresponding author, without restriction.

Code availability

The codes are available on a dedicated the Github repository: https://github.com/Nicolas-Latte/GANVC (https://doi.org/10.5281/zenodo.15480101[70]) or upon request to the corresponding author, without restriction.

References

1. Steffen, W. et al. Planetary boundaries: guiding human development on a changing planet. *Science* **347**, 6223 (2015).
2. IPCC. Climate Change 2022: Mitigation of Climate Change. Contribution of Working Group III to the Sixth Assessment Report of the Intergovernmental Panel on Climate Change. https://doi.org/10.1017/9781009157926. (2022)
3. Cross, A. T., Nevill, P. G., Dixon, K. W. & Aronson, J. Time for a paradigm shift toward a restorative culture. *Restor. Ecol.* **27**, 924–928 (2019).
4. Bastin, J.-F. et al. The global tree restoration potential. *Science* **365**, 76–79 (2019).
5. Lewis, S. L., Wheeler, C. E., Mitchard, E. T. A. & Koch, A. Restoring natural forests is the best way to remove atmospheric carbon. *Nature* **568**, 25–28 (2019).
6. Moore, J. W. & Schindler, D. E. Getting ahead of climate change for ecological adaptation and resilience. *Science* **376**, 1421–1426 (2022).
7. Veldman, J. W. et al. Tyranny of trees in grassy biomes. *Science* **347**, 484–485 (2015).
8. Parr, C. L., Te Beest, M. & Stevens, N. Conflation of reforestation with restoration is widespread. *Science* **383**, 698–701 (2024).
9. Bastin, J.-F. et al. Response to comments on "the global tree restoration potential". *Science* **366**, eaaz0493 (2019).
10. Friedlingstein, P., Allen, M., Canadell, J. G., Peters, G. P. & I., S. S. Comment on "The global tree restoration potential" by Bastin, et al. *Science* **366** (2019).
11. Hoek van Dijke, A. J. et al. Shifts in regional water availability due to global tree restoration. *Nat. Geosci.* **155**, 363–368 (2022).
12. Veldman, J. W. et al. Comment on 'The global tree restoration potential'. *Science* **366** (2019).
13. Pedersen, P. B. M., Ejrnæs, R., Sandel, B. & Svenning, J. C. Trophic rewilding advancement in anthropogenically impacted landscapes (TRAAIL): a framework to link conventional conservation management and rewilding. *Ambio* **49**, 231–244 (2020).
14. Perring, M. P. et al. Advances in restoration ecology: rising to the challenges of the coming decades. *Ecosphere* **6**, 131 (2015).
15. Stein, A., Gerstner, K. & Kreft, H. Environmental heterogeneity as a universal driver of species richness across taxa, biomes and spatial scales. *Ecol. Lett.* **17**, 866–880 (2014).
16. Buisson, E., Archibald, S., Fidelis, A. & Suding, K. N. Ancient grasslands guide ambitious goals in grassland restoration. *Science* **377**, 594–598 (2022).
17. Veldman, J. W. Clarifying the confusion: old-growth savannahs and tropical ecosystem degradation. *Philos. Trans. R. Soc. B Biol. Sci.* **371**, 20150306 (2016).
18. Bond, W. J. Out of the shadows: ecology of open ecosystems. *Plant Ecol. Divers.* **14**, 205–222 (2021).
19. Erdős, L. et al. How climate, topography, soils, herbivores, and fire control forest–grassland coexistence in the Eurasian forest-steppe. *Biol. Rev.* **97**, 2195–2208 (2022).
20. Garcia, A. et al. The global forest transition as a human affair. *One Earth* **2**, 417–428 (2020).
21. Suding, K. N., Gross, K. L. & Houseman, G. R. Alternative states and positive feedbacks in restoration ecology. *Trends Ecol. Evol.* **19**, 46–53 (2004).
22. Hobbs, R. J. et al. Managing the whole landscape: historical, hybrid, and novel ecosystems. *Front. Ecol. Environ.* **12**, 557–564 (2014).
23. Song, X.-P. et al. Global land change from 1982 to 2016. *Nature* **560**, 639–643 (2018).
24. Fløjgaard, C., Pedersen, P. B. M., Sandom, C. J., Svenning, J. C. & Ejrnæs, R. Exploring a natural baseline for large-herbivore biomass in ecological restoration. *J. Appl. Ecol.* **59**, 18–24 (2022).
25. Li, W. et al. Human fingerprint on structural density of forests globally. *Nat. Sustain. 2023* **64**, 368–379 (2023).
26. Jones, K. R. et al. One-third of global protected land is under intense human pressure. *Science* **360**, 788–791 (2018).
27. Valavi, R., Elith, J., Lahoz-Monfort, J. J. & Guillera-Arroita, G. blockCV: An r package for generating spatially or environmentally separated folds for k-fold cross-validation of species distribution models. *Methods Ecol. Evol.* **10**, 225–232 (2019).
28. Meyer, H. & Pebesma, E. Machine learning-based global maps of ecological variables and the challenge of assessing them. *Nat. Commun. 2022* **131**, 1–4 (2022).
29. Milà, C., Mateu, J., Pebesma, E. & Meyer, H. Nearest neighbour distance matching Leave-One-Out Cross-Validation for map validation. *Methods Ecol. Evol.* **13**, 1304–1316 (2022).
30. Pearce, E. A. et al. Substantial light woodland and open vegetation characterized the temperate forest biome before Homo sapiens. *Sci. Adv.* **9**, eadi9135 (2023).
31. Guirado, E. et al. Climate legacies drive the distribution and future restoration potential of dryland forests. *Nat. plants* **8**, 879–886 (2022).
32. Vancutsem, C. et al. Long-term (1990–2019) monitoring of forest cover changes in the humid tropics. *Sci. Adv.* **7**, eabe1603 (2021).

33. Berzaghi, F., Zhu, D., Alroy, J. & Ciais, P. Trait-based mechanistic approach highlights global patterns and losses of herbivore biomass functional diversity. *Funct. Ecol.* **38**, 808–819 (2024).
34. Wang, L. et al. Tree cover and its heterogeneity in natural ecosystems is linked to large herbivore biomass globally. One Earth https://doi.org/10.1016/J.ONEEAR.2023.10.007. (2023).
35. Lundgren, E. J. et al. Functional traits—not nativeness—shape the effects of large mammalian herbivores on plant communities. *Science* **383**, 531–537 (2024).
36. Zhang, X. et al. GWL-FCS30: a global 30m wetland map with a fine classification system using multi-sourced and time-series remote sensing imagery in 2020. *Earth Syst. Sci. Data* **15**, 265–293 (2023).
37. Tölgyesi, C., Buisson, E., Helm, A., Temperton, V. M. & Török, P. Urgent need for updating the slogan of global climate actions from "tree planting" to "restore native vegetation". *Restor. Ecol.* **30**, e13594 (2022).
38. Daskalova, G. N. & Kamp, J. Abandoning land transforms biodiversity. *Science* **380**, 581–583 (2023).
39. Zimov, S. A. Pleistocene park: return of the mammoth's ecosystem. *Science* **308**, 796–798 (2005).
40. Gordon, C. E. et al. Elephant rewilding affects landscape openness and fauna habitat across a 92-year period. *Ecol. Appl.* **33**, e2810 (2023).
41. Mirzabaev, A., Sacande, M., Motlagh, F., Shyrokaya, A. & Martucci, A. Economic efficiency and targeting of the African Great Green Wall. *Nat. Sustain. 2021* **51**, 17–25 (2021).
42. Purves, D. & Pacala, S. Predictive models of forest dynamics. *Science* **320**, 1452–1453 (2008).
43. Davoli, M. et al. Megafauna diversity and functional declines in Europe from the Last Interglacial to the present. *Glob. Ecol. Biogeogr.* **00**, 1–14 (2023).
44. Prentice, K. C. Bioclimatic distribution of vegetation for general circulation model studies. *J. Geophys. Res. Atmos.* **95**, 11811–11830 (1990).
45. Sykes, M. T., Colin Prentice, I. & Laarif, F. Quantifying the impact of global climate change on potential natural vegetation. *Clim. Change* **41**, 37–52 (1999).
46. Stephenson, N. L. Climatic control of vegetation distribution: the role of the water balance. *Univ. Chicago J.* **135**, 649–670 (1990).
47. Bond, W. J. Large parts of the world are brown or black: A different view on the 'Green World' hypothesis. *J. Veg. Sci.* **16**, 261–266 (2005).
48. Pedersen, R. Ø, Faurby, S. & Svenning, J. C. Late-Quaternary megafauna extinctions have strongly reduced mammalian vegetation consumption. *Glob. Ecol. Biogeogr.* **32**, 1814–1826 (2023).
49. Smith, M. D. et al. Extreme drought impacts have been underestimated in grasslands and shrublands globally. *Proc. Natl. Acad. Sci. USA* **121**, e2309881120 (2024).
50. Kropf, C. M., Vaterlaus, L., Bresch, D. N. & Pellissier, L. Tropical cyclone risk for global ecosystems in a changing climate. *Nat. Clim. Chang. 2025* **151**, 92–100 (2025).
51. Bastin, J.-F. et al. The extent of forest in dryland biomes. *Science* **356**, 635–638 (2017).
52. Bey, A. et al. Collect Earth: land use and land cover assessment through augmented visual interpretation. *Remote Sens.* **8**, 1–24 (2016).
53. Bey, A. et al. Mapping smallholder and large-scale cropland dynamics with a flexible classification system and pixel-based composites in an emerging frontier of Mozambique. *Remote Sens. Environ.* **239**, 111611 (2020).
54. Schepaschenko, D. et al. Recent Advances in Forest Observation with Visual Interpretation of Very High-Resolution Imagery. *Surv. Geophys.* 1–24 https://doi.org/10.1007/s10712-019-09533-z. (2019).
55. Marius-Constantin, P., Balas, V. E., Perescu-Popescu, L. & Mastorakis, N. Multilayer perceptron and neural networks. *WSEAS Trans. Circuits Syst.* **8**, 579–588 (2009).
56. UNESCO. The World Database on Protected Areas. https://www.protectedplanet.net/c/world-database-on-protected-areas (2011).
57. Deblauwe, V. et al. Remotely sensed temperature and precipitation data improve species distribution modelling in the tropics. *Glob. Ecol. Biogeogr.* **25**, 443–454 (2016).
58. Fick, S. E. & Hijmans, R. J. WorldClim 2: new 1-km spatial resolution climate surfaces for global land areas. *Int. J. Climatol.* **37**, 4302–4315 (2017).
59. Copernicus Climate Change Service (C3S). ERA5: Fifth generation of ECMWF atmospheric reanalyses of the global climate. Copernicus Climate Change Service Climate Data Store (CDS). https://cds.climate.copernicus.eu/cdsapp#!/home (2017).
60. Harris, I., Osborn, T. J., Jones, P. & Lister, D. Version 4 of the CRU TS monthly high-resolution gridded multivariate climate dataset. *Sci. Data 2020* **71**, 1–18 (2020).
61. Karger, D. N. et al. CHELSA-W5E5: Daily 1gkm meteorological forcing data for climate impact studies. *Earth Syst. Sci. Data* **15**, 2445–2464 (2023).
62. Wan, Z. S. Hook, G. H. MODIS/Aqua land surface temperature/emissivity 8-day L3 global 1km SIN Grid V061. NASA EOSDIS Land Processes Distributed Active Archive Center https://doi.org/10.5067/MODIS/MYD11A2.061 (2021).
63. Hengl, T. et al. SoilGrids250m: Global gridded soil information based on machine learning. *PLoS One* **12**, e0169748 (2017).
64. Danielson, J. J. & Gesch, D. B. Global multi-resolution terrain elevation data 2010 (GMTED2010). Open-File Report https://pubs.er.usgs.gov/publication/ofr20111073 10.3133/OFR20111073. (2011).
65. Giglio, L. C. Justice L. Boschetti D. R. MODIS/Terra+Aqua burned area monthly L3 global 500m SIN Grid V061. NASA EOSDIS Land Processes Distributed Active Archive Center https://doi.org/10.5067/MODIS/MCD64A1.061. (2021).
66. Berzaghi, F., Zhu, D., Alroy, J. & Ciais, P. Global distribution of mammal herbivore biomass reveals megafauna extinction patterns. bioRxiv 2021.10464976 (2021).
67. Greenspoon, L. et al. The global biomass of wild mammals. *Proc. Natl. Acad. Sci. USA* **120**, e2204892120 (2023).
68. Olson, D. M. et al. Terrestrial ecoregions of the world: a new map of life on Earth. A new global map of terrestrial ecoregions provides an innovative tool for conserving biodiversity. *Bioscience* **51**, 933–938 (2001).
69. Thrasher, B., Maurer, E. P., McKellar, C. & Duffy, P. B. Technical Note: Bias correcting climate model simulated daily temperature extremes with quantile mapping. *Hydrol. Earth Syst. Sci.* **16**, 3309–3314 (2012).
70. Bastin, J.-F. et al. Global Alternatives of Natural Vegetation Cover, Zenodo. https://doi.org/10.5281/zenodo.15480101, 2025.

Acknowledgements

The authors would like to thank the following institutions for financial support: J.F.B. is supported by a start-up grant from the Francqui foundation (Belgium), P.D., Hd.L., A.V.D. are supported by the FNRS (Belgium); F.B. is supported by the European Union's Horizon 2020 Research and Innovation Program under Marie Sklodowska-Curie Grant 845265; F.T.M. acknowledges support by the King Abdullah University of Science and Technology (KAUST) and by the KAUST Climate and Livability Initiative; J.C.S. is supported by Danish National Research Foundation (grant DNRF173), Independent Research Fund Denmark | Natural Sciences (grant 0135-00225B), Y.U. is supported by ARES. T.B. is supported by AGRINATURA-ERAIFT consortium through the European Union-funded project DCI-ENV 2020/416-397 on "Capacity building of

biodiversity practitioners, scientists and policy makers for the sustainable management of protected areas and forest ecosystems in Africa". The authors would like also to add a special thanks to Cécile Rénier from UCLouvain from commenting the document. All data needed to evaluate the conclusions in the paper are present in the paper, in the Supplementary Materials, and on the Github repository: https://github.com/Nicolas-Latte/GANVC.

Author contributions

J.F.B. conceptualized the original idea of the study. N.L. and J.F.B. designed the modelling framework. N.L. wrote the scripts. J.F.B. and N.L. performed the analyses and controlled the replicability of the results. J.F.B. led the writing of the manuscript with the support of J.B., C.G., F.B., F.T.M., J.C.V., E.A., S.B., T.B., Sam B., T.W.C., Td.H., Hd.L., P.D., M.D., A.H.V.D., S.L., G.M., C.M., D.M., F.N.R., M.P., A.P., F.Q., O.R., K.R.S., B.S., Y.T., Y.U.S., A.V.L., P.L.

Competing interests

The authors declare no competing interests.

Additional information

Supplementary information The online version contains supplementary material available at https://doi.org/10.1038/s41467-025-61520-8.

Correspondence and requests for materials should be addressed to Jean-François Bastin.

Peer review information *Nature Communications* thanks the anonymous reviewers for their contribution to the peer review of this work. A peer review file is available.

[1]TERRA Teaching and Research Centre, Gembloux Agro-Bio Tech, Université de Liège, Gembloux, Belgium. [2]School of Agricultural, Forest and Food Sciences, Bern University of Applied Sciences, BFH-HAFL, Bern, Switzerland. [3]Department of Earth System Sciences, Institute of Terrestrial Ecosystems, ETH Zurich, Zurich, Switzerland. [4]World Maritime University, Malmö, Sweden. [5]Laboratory of Climate and Environmental Sciences, UMR - Commissariat a l'energie atomique (CEA), Gif-sur-Yvette, France. [6]Environmental Sciences and Engineering, Biological and Environmental Science and Engineering Division, King Abdullah University of Science and Technology, Thuwal, Kingdom of Saudi Arabia. [7]Center for Ecological Dynamics in a Novel Biosphere (ECONOVO), Department of Biology, Aarhus University, Aarhus, Denmark. [8]Faculté d'Agronomie, Université de Parakou, Parakou, Benin. [9]Department of Plant and Soil Sciences, University of Pretoria, Pretoria, South Africa. [10]UFR Environnement, Université Jean Lorougnon Guédé, Daloa, Ivory Coast. [11]Ecole Régionale Post-Universitaire d'Aménagement et Gestion Intégrés des Forêts et Territoires Tropicaux (ERAIFT), Kinshasa, DRC, Republic of the Congo. [12]Institute of Integrative Biology, ETH Zurich, Zurich, Switzerland. [13]Q-Forestlab, Faculty of Bioscience Engineering, Ghent University, Belgium. [14]Louis Bolk Institute, AJ Bunnik, The Netherlands. [15]Institut des Sciences de la forêt tempérée (ISFORT), Université du Québec à Montréal (UQAM), Montreal, Canada. [16]Centre d'Étude de la forêt (CEF), Université du Québec en Outaouais (UQO), Outaouais, Canada. [17]UN-FAO Climate Change Office, Rome, Italy. [18]ESSA-Forêts, Université d'Antananarivo, Antananarivo, Madagascar. [19]INRAE, UMR1391 ISPA, Université de Bordeaux, Bordeau, France. [20]Rewilding Europe, Nijmegen, The Netherlands. [21]University of Lubumbashi, Faculty of Architecture, Lubumbashi, DRC, Republic of the Congo. [22]TERN, School of Biological Sciences, The University of Adelaide, Adelaide, Australia. [23]Unité Ecologie, Restauration Ecologique et Paysage, Faculté des Sciences Agronomiques, Université de Lubumbashi, Lubumbashi, DRC, Democratic Republic of the Congo. ✉e-mail: jfbastin@uliege.be